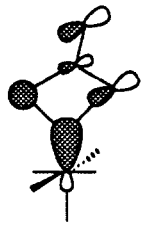

The small kinetic isotope effect (k_H/k_D = 1.13) observed for the decarboxylation reaction is indicative of an early transition state for hydrogen transfer from the carbon atom of the formate ligand to the metal center. This observation is consistent with Bo and Dedieu's calculations[5] which reveal significant C-H interaction in the adduct formed prior to the CO_2 insertion process. For example, the C-H distance in the proposed adduct $[Cr(CO)_5H\cdots CO_2]^-$ of 1.15 Å is quite close to the anticipated value in the formate ligand.[19] On the other hand in instances involving a less hydridic hydride ligand where adduct formation should be less significant, a larger kinetic isotope effect would be expected. This is indeed observed in the kinetic isotope effect (k_H/k_D = 1.55) for the decarboxylation of η^5-$C_5H_5)Re(O_2CH)(NO)PPh_3$.[20]

Acknowledgment. The financial supprt of this research by the National Science Foundation (Grant CHE 88-17873) and the Robert A. Welch Foundation is greatly appreciated.

(19) Darensbourg, D. J.; Day, C. S.; Fischer, M. B. *Inorg. Chem.* **1981**, *20*,. 3577.
(20) Merrifield, J. H.; Gladysz, J. A. *Organometallics* **1983**, *2*, 782.

Single-Crystal, Solid-State, and Solution ^{113}Cd NMR Studies of $[Cd(SR)_2(N\text{-donor})_2]$ Complexes. Structural and Spectroscopic Analogues for Biologically Occurring $[M(S\text{-Cys})_2(His)_2]$ Centers

Rodolfo A. Santos, Eric S. Gruff, Stephen A. Koch,* and Gerard S. Harbison*

Contribution from the Department of Chemistry, State University of New York at Stony Brook, Stony Brook, New York 11794-3400. *Received March 13, 1990*

Abstract: A series of compounds of the formula $[Cd(SR)_2(N\text{-donor})_2]$ has been synthesized, characterized by X-ray crystallography, and studied by solid-state and solution ^{113}Cd NMR spectroscopy to serve as analogues for biologically occurring $[M(S\text{-Cys})_2(His)_2]$ centers. The compounds include $[Cd(S\text{-}2,4,6\text{-}i\text{-}Pr_3\text{-}C_6H_2)_2(bpy)]$ (**1**), $[Cd(S\text{-}2,4,6\text{-}i\text{-}Pr_3\text{-}C_6H_2)_2(phen)]_2$ (**2**), $[Cd(S\text{-}2,4,6\text{-}i\text{-}Pr_3\text{-}C_6H_2)_2(1\text{-Me-imid})_2]$ (**3**), and $[Cd(S\text{-}2,4,6\text{-}i\text{-}Pr_3\text{-}C_6H_2)_2(1,2\text{-}Me_2\text{-imid})_2]$ (**4**). Compounds **1**-**3** have been characterized by X-ray crystallography. The unit cell parameters are as follows. For **1**: a = 15.081 (9) Å, b = 14.716 (9) Å, c = 17.72 (1) Å, β = 100.36 (5)°, V = 3868 (8) Å^3, Z = 4, $P2_1/c$. For **2**: a = 10.12 (2) Å, b = 16.56 (1) Å, c = 23.50 (2) Å, β = 92.1 (5)°, V = 3934 (14) Å^3, Z = 2, $P2_1/n$. For **3**: a = 16.541 (7) Å, b = 15.887 (6) Å, c = 16.36 (1) Å, β = 108.91 (5)°, V = 4068 (7) Å^3, Z = 4, $P2_1/c$. Compounds **1**-**4** have been characterized by solution and CP/MAS ^{113}Cd spectroscopy. The ^{113}Cd shielding tensors of **1** have been obtained from a single-crystal study (σ_{11} = 814 ppm, σ_{22} = 630 ppm, σ_{33} = 32 ppm). Similar large chemical shielding anisotropies (CSA) were also observed for **2**-**4**. The solution ^{113}Cd NMR spectra are consistent with monomeric $[Cd(SR)_2(N)_2]$ structures. The large difference in the ^{113}Cd chemical shift for **2** in the solution and solid state is explained by the weak dimeric structure of **2** in the solid state. The implications of the large CSA to solution and solid-state measurements of related centers in proteins are discussed.

Recently, a wide variety of metalloproteins containing or believed to contain a $[Zn(S\text{-Cys})_2(His)_2]$ site have been discovered.[1] Prominent in this group are a major class of the "zinc finger" proteins, which include transcription factor IIIA (TFIIIA)[1,2] and, most recently, in the human immunodeficiency virus type 1 enhancer binding protein (HIV-EP1).[3] This coordination center had previously been observed in the imidazole-inhibited active site of liver alcohol dehydrogenase (LADH).[4] Since zinc is a spectroscopically silent metal, cadmium and cobalt complexes have been substituted in the native proteins to further aid in the study of the spectroscopic features of zinc centers.[5] We have been synthesizing and studying the properties of a series of potential models, $[M(SR)_x(N\text{-donor})_{(4-x)}]$ (M = Zn, Co, Cd) for cysteine-containing zinc metalloproteins.[6]

Cadmium is often substituted in the proteins and used to aid in the determination of the coordination environment of the native metal, primarily because of the usefulness of ^{113}Cd NMR.[7,8] The chemical shift range of ^{113}Cd NMR exceeds 900 ppm and the technique is widely regarded as one of the most useful methods for aiding in the determination of the coordination sphere of a wide range of cadmium compounds. It has been shown that the trends in proteins for chemical shift vs ligand type follow those seen for simple coordination complexes [i.e., thiolate ligands are most strongly deshielding, while nitrogen and oxygen donor ligands have a weaker deshielding effect on the Cd(II) ion], but the effect of coordination number, geometric distortions, and ligand charge

(1) (a) Klug, A.; Rhodes, D. *Trends Biochem. Sci.* **1987**, *12*, 464. (b) Evans, R. M.; Hollenberg, S. M. *Cell* **1988**, *52*, 1. (c) Berg, J. M. *Prog. Inorg. Chem.* **1989**, *37*, 143.
(2) Miller, J.; McLachlan, A. D.; Klug, A. *EMBO J.* **1985**, *4*, 1609.
(3) van Wijnen, A. J.; Wright, K. L.; Lian, J. B.; Stein, J. L.; Stein, G. S. *J. Biol. Chem.* **1989**, *264*, 15034.
(4) Ekland, H.; Samama, J.-P.; Wallén, L. *Biochemistry* **1982**, *21*, 4858.
(5) Vallee, B. L. In *Zinc Proteins*; Spiro, T. G., Ed.; Wiley-Interscience: New York, 1983.
(6) (a) Corwin, D. T., Jr.; Fikar, R.; Koch, S. A. *Inorg. Chem.* **1987**, *26*, 3079. (b) Corwin, D. T., Jr.; Gruff, E. S.; Koch, S. A. *J. Chem. Soc., Chem. Commun.* **1987**, 966. (c) Corwin, D. T., Jr.; Gruff, E. S.; Koch, S. A. *Inorg. Chim. Acta* **1988**, *151*, 5. (d) Corwin, D. T., Jr.; Koch, S. A. *Inorg. Chem.* **1988**, *27*, 493. (e) Gruff, E. S.; Koch, S. A. *J. Am. Chem. Soc.* **1989**, *111*, 8762.
(7) Summers, M. F. *Coord. Chem. Rev.* **1988**, *86*, 43.
(8) Olvos, J. D.; Armitage, I. M. In *Biochemical Structure Determination by NMR*; Marcel Dekker: New York, 1982.

0002-7863/90/1512-9257$02.50/0

Table I. X-ray Crystallographic Parameters

	[Cd(S-2,4,6-*i*-Pr_3-C_6H_2)$_2$(bpy)] (**1**)	[Cd(S-2,4,6-*i*-Pr_3-C_6H_2)$_2$(phen)]$_2$ (**2**)	Cd(S-2,4,6-*i*-Pr_3-C_6H_2)$_2$(1-Me-imid)$_2$ (**3**)
formula	$CdS_2N_2C_{40}H_{54}$	$Cd_2S_4N_4C_{84}H_{108}$	$CdS_2N_4C_{38}H_{58}$
formula wt	739.4	1526.8	747.4
a, Å	15.081 (9)	10.12 (2)	16.541 (7)
b, Å	14.716 (9)	16.56 (1)	15.887 (6)
c, Å	17.72 (1)	23.50 (2)	16.36 (1)
α, deg	90.00	90.00	90.00
β, deg	100.36 (5)	92.1 (1)	108.91 (5)
γ, deg	90.00	90.00	90.00
V, Å^3	3868 (8)	3934 (14)	4068 (7)
Z	4	2	4
d_{calc}, g cm^{-3}	1.27	1.29	1.22
space group	$P2_1/c$	$P2_1/n$	$P2_1/c$
temperature	ambient	ambient	ambient
radiation, Å	Mo Kα (0.71073)	Mo Kα (0.71073)	Mo Kα (0.71073)
lin. abs coeff, cm^{-1}	6.95	6.86	6.63
scan mode	$\theta/2\theta$	$\theta/2\theta$	$\theta/2\theta$
$2\theta_{max}$, deg	52	50	42
no. of obsvatns	3084	3145	2452
no. of variables	406	424	406
R	0.045	0.052	0.039
R_w	0.052	0.062	0.044
ESD of unit wt obsvatn	1.35	1.56	2.33

are not yet fully understood. Since the single-crystal ^{113}Cd NMR spectrum of a protein or model compound reflects the effect of a quantified set of ligands, comparison with dissolved species and eventually to Cd-substituted metalloproteins should provide greater insight into these often subtle effects. Early studies of single crystals using ^{113}Cd NMR, including $Cd(NO_3)_2{\cdot}8H_2O$ and $CdSO_4{\cdot}8H_2O$ and a monohydrated form of cadmium glycinate, helped to establish some of the basic correlations between the cadmium chemical shielding orientation and the structural features of the complexes.[9] More recent work has extended these studies to other systems and to proteins.[10]

By cross polarizing the ^{113}Cd nucleus (12.26% natural abundance) to abundant spins (e.g., ^{1}H), the sensitivity of a solid-state sample can be amplified by a maximum of 4.5 times [$\gamma(^1H)/\gamma(^{113}Cd)$].[11,12] Furthermore, the resolution of a powdered sample can be increased by combining the cross-polarization technique with magic-angle spinning (CP/MAS).[13]

We present here the solution and solid-state ^{113}Cd NMR studies of the compounds [Cd(S-2,4,6-*i*-Pr_3-C_6H_2)$_2$(bpy)] (**1**), [Cd(S-2,4,6-*i*-Pr_3-C_6H_2)$_2$(phen)] (**2**), [Cd(S-2,4,6-*i*-Pr_3-C_6H_2)$_2$(1-Me-imid)$_2$] (**3**), and [Cd(S-2,4,6-*i*-Pr_3-C_6H_2)$_2$(1,2-Me_2-imid)$_2$] (**4**).[21] The coordination centers of **1**–**4** are intended to serve as more readily studied models for the [Zn(*S*-Cys)$_2$(His)$_2$] sites mentioned above. These allow evaluation of the influence of the shielding tensor both on the solid-state NMR spectra of such metal-binding sites and on the solution NMR properties, specifically chemical shielding anisotropy induced relaxation.

To our knowledge, compound **1** is the highest molecular weight compound studied to date by single-crystal NMR. The crystal structure and solution ^{113}Cd NMR spectrum of **3** was previously communicated.[6b]

Table II. Selected Bond Distances (Å) and Angles (deg) for Cd(S-2,4,6-*i*-Pr_3-C_6H_2)$_2$(bpy) (**1**)

Cd–S(1)	2.417 (2)	Cd–N(1)	2.334 (6)
Cd–S(2)	2.436 (2)	Cd–N(2)	2.337 (6)
Cd–S(1)–C(11)	98.2 (2)	S(1)–Cd–N(2)	111.7 (2)
Cd–S(2)–C(21)	100.9 (20	S(2)–Cd–N(1)	104.5 (2)
S(1)–Cd–S(2)	125.99 (7)	S(2)–Cd–N(2)	114.0 (2)
S(1)–Cd–N(1)	116.7 (2)	N(1)–Cd–N(2)	70.4 (2)

Experimental Section

Preparation of Compounds. [Cd(S-2,4,6-*i*-Pr_3-C_6H_2)$_2$(bpy)] (1). A 1.55-g (6.4 mmol) sample of lithium thiolate was dissolved in 35 mL of methanol and 0.58 g (3.2 mmol) of $CdCl_2$ added under N_2. Next, 0.50 g (3.2 mmol) of 2,2′-bipyridine was added, resulting in an immediate color change to lemon yellow. A hot (50 °C) filtration, followed by cooling of the solution to −20 °C, resulted in precipitation of 2.09 g (89%) of bright yellow product. ^{1}H NMR ($CDCl_3$): 0.99 (d, 24 H, *o*-CH_3), 1.17 (d, 12 H, *p*-CH_3), 2.73 (m, 2 H, *p*-H), 3.90 (m, 4 H, *o*-CH), 6.66 (s, 4 H, *m*-H), 7.2–8.0 (m, 8 H, bpy) ppm.

[Cd(S-2,4,6-*i*-Pr_3-C_6H_2)$_2$(phen)]$_2$ (2). LiSR 1.03 g, 4.2 mmol, $CdCl_2$ (0.32 g, 1.7 mmol), and phen (0.31 g, 1.7 mmol) were combined in 25 mL of absolute ethanol. The ethanol was removed after stirring for 30 min and the crude yellow solid recrystallized from CH_2Cl_2/hexane. Yield 0.76 g (57%). ^{1}H NMR ($CDCl_3$): 0.88 (d, 24 H, *o*-CH_3), 1.15 (d, 12 H, *p*-CH_3), 2.71 (m, 2 H; *p*-CH), 3.88 (m, 4 H, *o*-CH), 6.60 (s, 4 H, *m*-H), 7.52 (dd, 2 H, 3,8-H), 7.86 (s, 2 H, 5,6-H), 8.08 (dd, 2 H, 4,7-H), 8.32 (dd, 2 H, 2,9-H) ppm.

[Cd(2,4,6-*i*-Pr_3-C_6H_2)$_2$(1-Me-imid)$_2$] (3). LiSR (1.02 g, 4.2 mmol) and $CdCl_2$ (0.39 g, 2.1 mmol) were combined in absolute ethanol and 1-Me-imid (0.70 mL) was added with a syringe. The resultant white precipitate was filtered and subsequently recrystallized from hot CH_3CN. The yield of **3** was 1.40 g (93%). ^{1}H NMR ($CDCl_3$): 1.04 (d, 24 H, *o*-CH_3), 1.23 (d, 12 H, *p*-CH_3), 2.83 (m, 2 H, *p*-CH), 3.55 (s, 6 H, 1-CH_3), 4.22 (m, 4 H, *o*-CH), 6.59 (s, 4 H, *m*-H), 6.84 (s, 2 H, 2-H), 6.7–6.9 (m, 4 H, 4,5-H) ppm.

[Cd(S-2,4,6-*i*-Pr_3-C_6H_2)$_2$(1,2-Me_2-imid)$_2$] (4). Compound **4** can be prepared in 70% yield by using the same procedure as for the 1-Me-imid analogue.

X-ray Crystal Structures. Unit cell determinations and data collection were performed by on a CAD4 diffractometer using standard procedures

(9) (a) Honkonen, R. S.; Doty, F. D.; Ellis, P. D. *J. Am. Chem. Soc.* **1983**, *105*, 4163. (b) Honkonen, R. S.; Ellis, P. D. *J. Am. Chem. Soc.* **1984**, *106*, 5488. (c) Honkonen, R. S.; Marchetti, P. S.; Ellis, P. D. *J. Am. Chem. Soc.* **1986**, *108*, 912.

(10) (a) Rivera, E.; Kennedy, M. A.; Adams, R. H.; Ellis, P. D. *J. Am. Chem. Soc.* **1990**, *112*, 1400. (b) Ellis, P. D. *J. Biol. Chem.* **1989**, *264*, 3108.

(11) Hartmann, S. R.; Hahn, E. L. *J. Phys. Rev.* **1962**, *128*, 2042.

(12) Pines, A.; Gibby, M. G.; Waugh, J. S. *J. Chem. Phys.* **1973**, *59*, 569.

(13) Cheung, T. T. P.; Worthington, L. E.; Murphy, D. D.; Gerstein, B. C. *J. Magn. Reson.* **1980**, *41*, 158.

(14) Maelia, L. E.; Koch, S. A. *Inorg. Chem.* **1986**, *25*, 1896.

(15) (a) Mehring, M. *High Resolution NMR in Solids*; Springer: Berlin, 1983; Chapter 2. (b) Santos, R. A.; Tang, P.; Chien, W.-J.; Kwan, S.; Harbison, G. S. *J. Phys. Chem.* **1990**, *94*, 2717.

(16) Crosby, G. A.; Highland, R. G.; Truesdell, K. A. *Coord. Chem. Rev.* **1985**, *64*, 41.

(17) Henry, N. F. M.; Lonsdale, K., Eds. *International Tables for X-ray Crystallography*; Kynoch Press: Birmingham, England, 1952; Vol. 1.

(18) Herzfeld, J.; Berger, A. E. *J. Chem. Phys.* **1980**, *73*, 6021.

(19) (a) Bobsein, B. R.; Myers, R. J. *J. Am. Chem. Soc.* **1980**, *102*, 2454. (b) Bobsein, B. R.; Myers, R. J. *J. Biol. Chem.* **1981**, *256*, 5313. (c) South, T. L.; Kim, B.; Summers, M. F. *J. Am. Chem. Soc.* **1989**, *111*, 395.

(20) Ellis, P. D. *The Multinuclear Approach to NMR Spectroscopy*; Lambert, J. B., Riddell, F. G., Eds.; D. Reidel: Dordrecht, The Netherlands, 1983; Chapter 22.

(21) Abbreviations: S-2,4,6-*i*-$Pr_3C_6H_2$, 2,4,6-triisopropylbenzenethiolate; S-2,3,5,6-Me_4C_6H, 2,3,5,6-tetramethylbenzenethiolate; bpy, 2,2′-bipyridine; phen, 1,10-phenanthroline; 1-Me-imid, 1-methylimidazole; 1,2-Me_2-imid, 1,2-dimethylimidazole.

Table III. Selected Bond Distances (Å) and Angles (deg) for $[Cd(S\text{-}2,4,6\text{-}i\text{-}Pr_3\text{-}C_6H_2)_2(phen)]_2$ (**2**)

Cd-S(1)	2.454 (3)	Cd-N(2)	2.395 (8)
Cd-S(2)	2.474 (4)	Cd-S(2)′	3.066 (3)
Cd-N(1)	2.364 (8)	Cd-Cd′	4.349 (5)
Cd-S(2)-Cd′	102.9 (1)	S(2)-Cd-N(1)	112.8 (2)
Cd-S(1)-C(11)	102.6 (3)	S(2)-Cd-N(2)	100.3 (2)
Cd-S(2)-C(21)	105.6 (3)	N(1)-Cd-N(2)	69.6 (3)
Cd-S(2)′-C(21)′	142.8 (3)	S(1)-Cd-S(2)′	95.6 (1)
S(1)-Cd-S(2)	134.7 (1)	S(1)-Cd-S(2)′	77.1 (1)
S(1)-Cd-N(1)	111.7 (2)	N(1)-Cd-S(2)′	89.0 (2)
S(1)-Cd-N(2)	102.6 (2)	N(2)-Cd-S(2)′	155.8 (2)

Table IV. Selected Bond Distances (Å) and Angles (deg) for $[Cd(S\text{-}2,4,6\text{-}i\text{-}Pr_3\text{-}C_6H_2)_2(1\text{-}Me\text{-}imid)_2]$ (**3**)

Cd-S1	2.471 (3)	Cd-N1	2.259 (9)
Cd-S2	2.451 (3)	Cd-N2	2.268 (9)
S1-Cd-S2	126.1 (1)	S2-Cd-N2	110.0 (3)
S1-Cd-N1	103.8 (3)	S2-Cd-N1	111.0 (3)
S1-Cd-N2	107.1 (3)	N1-Cd-N2	94.0 (4)
Cd-S1-C11	101.3 (3)	Cd-S2-C21	101.5 (3)

previously described.[14] Parameters connected with the crystallographic studies are given in Table I.

$[Cd(S\text{-}2,4,6\text{-}i\text{-}Pr_3C_6H_2)_2(bpy)]$ (1). Yellow crystals were grown by slowing cooling a hot (60 °C) acetonitrile solution to room temperature. A piece measuring 0.5 × 0.5 × 0.4 mm was cut from a larger crystal and glued to a glass fiber with epoxy resin. The unit cell parameters and the systematic absences [$(h0l(l = 2n)$ and $0k0$ $(k = 2n)$] indicated the monoclinic space group $P2_1/c$ (No. 14).

The crystal structure of **1** was solved with the TEXRAY structure solution software package (Molecular Structure Corp.). The position of the cadmium atom was determined from an origin-removed Patterson map and the other non-hydrogen atoms located and refined by using difference maps followed by least-squares cycles. Both decay and absorption corrections were applied and after calculation of the hydrogen atom positions and a full anisotropic refinement of the structure, a final R (R_w) value of 0.045 (0.052) was obtained. Atomic positional parameters are given in the supplementary material and bond distances and angles are found in Table II.

$[Cd(S\text{-}2,4,6\text{-}i\text{-}Pr_3C_6H_2)_2(phen)]_2$ (2). Crystals were grown by cooling a toluene solution to room temperature. A yellow crystal measuring 0.3 × 0.2 × 0.5 mm was glued to a glass fiber with epoxy resin. Unit cell parameters and the systematic absences indicated the monoclinic space group $P2_1/n$ (No. 14).

The position of the cadmium atom was determined from an origin-removed Patterson map and the other non-hydrogen atoms located and refined by using difference maps followed by least-squares cycles. Both decay and absorption corrections were applied and after calculation of the hydrogen atom positions and a full anisotropic refinement of the structure, a final R value of 0.052 and R_w of 0.062 were obtained. Atomic coordinates are given in the supplementary material and selected bond distance and angles are given in Table III.

$[Cd(S\text{-}2,4,6\text{-}i\text{-}Pr_3C_6H_2)_2(1\text{-}Me\text{-}imid)_2]$ (3). A crystal was grown from a slowly cooled acetonitrile solution and mounted on a glass fiber with epoxy. The unit cell and systematic absences indicated the monoclinic space group $P2_1/c$ (No. 14).

An origin-removed Patterson map was used to locate the cadmium atom, while the remaining heavy atoms were located by using difference Fourier maps and refined by using least-squares cycles. The structure converged with an R of 0.039 and R_w of 0.044, after the hydrogen atoms (except the imidazole methyl protons, for which one was located on a difference map and the others calculated). Atomic coordinates are given in the supplementary material and bond distances and angles are given in Table IV.

Solution ^{113}Cd NMR Spectroscopy. Samples were prepared by dissolving the compounds in the appropriate solvents and filtering the solution into a 10 mm × 4.75 mm sample tube (homemade). ^{113}Cd NMR spectra were recorded on a Bruker MSL-400 spectrometer operating at 88.8 MHz with a high-power solenoidal single-coil probe. A pulse time of 8 μs was used with an 8-s recycle delay and a digitization rate of 40 kHz. Typically, between 100 and 400 transients were acquired (depending on concentration of the samples) and after a baseline correction to remove any AC component, line broadening was applied (equal to the half-height line width of the peak), followed by a Fourier transform of the free induction decay (FID). Early studies were done with a GE/Nicolet NT300 spectrometer operating at 66.6 MHz.

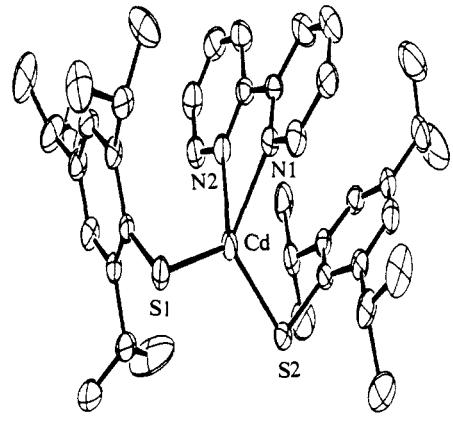

Figure 1. Structure of $[Cd(S\text{-}2,4,6\text{-}i\text{-}Pr_3\text{-}C_6H_2)_2(bpy)]$ (**1**).

Solid-State ^{113}Cd NMR. All solid-state spectra were run on a home-built spectrometer operating at 7.1 T (corresponding to a ^1H frequency of 301.4 MHz). The spectrometer frequency was set to 66.88 MHz and the 90° pulse determined to be 4.5 μs. The instrument was calibrated with a sample of solid $Cd(NO_3)_2{\cdot}4H_2O$ obtained commercially (Aldrich Chemical Co.). Spectra were obtained by use of a standard cross-polarization pulse sequence[12] with a Hartmann-Hahn contact time of 3 ms and matched radio frequency fields corresponding to rotating-frame frequencies of 55 kHz. The rf field strength is large compared with the largest instantaneous off-resonance frequencies encountered in these studies (~400 ppm or 27 kHz); in addition, such off-resonance effects are partially averaged by sample rotation. Recycle delays were typically 8 s and 512 transients were acquired, yielding adequate signal to noise for the spectra. All solid-state spectra were referenced to an external 0.1 M aqueous $Cd(ClO_4)_2$ standard.

Single crystals (volume ~25–30 mm^3) of **1** were grown from a slowly evaporated acetonitrile solution. Crystals were analyzed for structural flaws by polarization microscopy, and the faces of the crystal were subsequently indexed by using an optical goniometer. The crystal was mounted in a glass support cell and placed on the goniometer head of a probe of double-resonance circuitry. Three mutually orthogonal 360° rotation plots were taken in 14° increments (512 transients were obtained per increment). Although only two orthogonal rotation plots are required to determine shielding tensors for this space group, the third plot was obtained for completeness and served as a check on the results. Peak positions were obtained by three-point fits to the maxima of the resonance lines and shielding tensors were obtained by standard methods.[15]

CP/MAS spectra were obtained at several rotor speeds between 3.4 and 4.53 kHz. Contact times were 3 ms and the magic angle was adjusted for minimum line width on a sample of solid $Cd(NO_3)_2{\cdot}4H_2O$. A recycle delay of 12 s was used, the sweep width was 0.1 MHz, and 2048 points were collected per transient.

Results

Synthesis and Solid-State Structure. The synthesis of $[Cd(SR)_2(N\text{-donor})_2]$ compounds is readily accomplished in good yield by combining appropriate amounts of LiSR, $CdCl_2$, and N-donor ligand in acetonitrile or toluene. Large single crystals of **1–3** were grown by slow evaporation or cooling of solutions and showed no evidence of twinning or other defects. Compounds **1** and **2** are yellow due to interligand transmetallic charge-transfer (ITCT) bands from the thiolate ligands to empty π^* orbitals on the bpy or phen ligand.[16] All the compounds show unremarkable ^1H NMR spectra with small shifts (<0.1 ppm) due to the presence of the Cd(II) ion.

Figure 1 shows the structure of $[Cd(S\text{-}2,4,6\text{-}i\text{-}Pr_3\text{-}C_6H_2)_2(bpy)]$. The $Cd\text{-}S_{av}$ [2.43 (1) Å] and $Cd\text{-}N_{av}$ [2.336 (2) Å] distances are unremarkable and the angular distortions around the cadmium atom [S-Cd-S 125.99 (7)°, S-Cd-N_{av} 112°, N-Cd-N 70.4 (2)°] are presumably due to the small "bite angle" of the bpy ligand and the mutual repulsion between the thiolate ligands. There is no interaction between adjacent molecules in the unit cell and the geometry about the cadmium(II) ion may be regarded as distorted tetrahedral.

The corresponding phenanthroline complex, **2**, shows an unexpected dissimilarity to **1**. Instead of four monomeric units expected in the space group $P2_1/n$, each unit cell contains two weakly bridged $[Cd(SR)_2(phen)]_2$ dimers (Figure 2). The Cd_2S_2

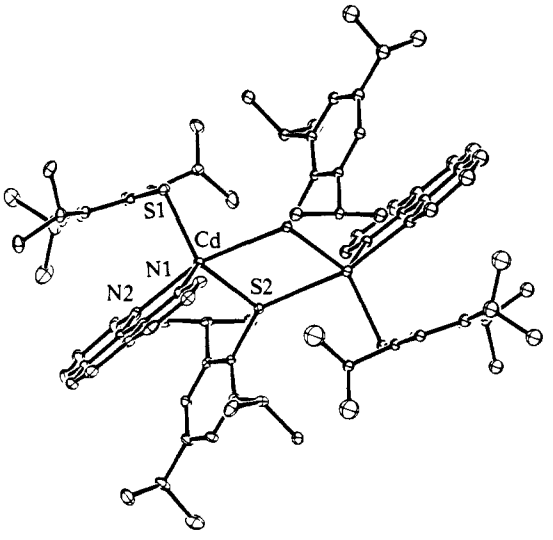

Figure 2. Structure of $[Cd(S\text{-}2,4,6\text{-}i\text{-}Pr_3\text{-}C_6H_2)_2(phen)]_2$ (2).

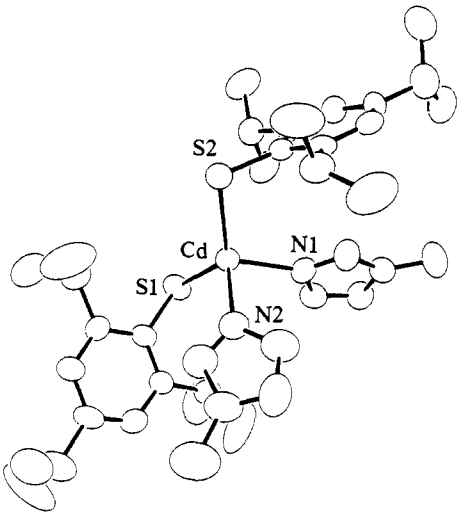

Figure 3. Structure of $[Cd(S\text{-}2,4,6\text{-}i\text{-}Pr_3\text{-}C_6H_2)_2(1\text{-}Me\text{-}imid)_2]$ (3).

bridging unit is quite asymmetric with Cd–S2′ = 3.066 (3) Å and Cd–S2 = 2.474 (4) Å. The Cd_2S_2 unit, which is planar because of the center of symmetry, has S2–Cd–S2′ 77.1 (1)° and Cd–S2–Cd′ 102.9 (1)°. The terminal Cd–S bond distance [Cd–S1 2.454 (3) Å] is only slightly shorter than the Cd–S2 bridging distance. The long Cd–Cd distance [4.349 (5) Å] provides further evidence of a very weak dimer in the solid state. The Cd–N distances [2.364 (8) and 2.395 (8) Å] are slightly longer than for 1. The angles about the cadmium atom indicate a distorted trigonal-bipyramidal geometry, where S(1), S(2), and N1 make up the equatorial plane [the sum of S1–Cd–S2 (134.7 (1)°), S1–Cd–N1 (111.7 (2)°), and S2–Cd–N1 (112.8 (2)°) is 359.2°]. The axial ligands are provided by S2′ [with the long Cd–S2′ distance of 3.066 (3) Å and N2; the N2–Cd–S2′ angle is 155.8 (2)°].

The solid-state structure of 3 is unremarkable, with four discrete $[Cd(SR)_2(1\text{-}Me\text{-}imid)_2]$ molecules in each unit cell (Figure 3).[6b] The Cd–S_{av} [2.46 (1) Å] and Cd–N_{av} [2.264 (9) Å] distances are quite similar to 1, but the angles [S–Cd–S 126.1 (1)°, S–Cd–N 104–111°, and N–Cd–N 94.0 (4)°] are closer to 109.5° due to the lack of a chelating ligand. The crystal structure of 4 was not determined, but is likely to be quite similar to that of 3.

Solution ^{113}Cd Nuclear Magnetic Resonance Studies. The solution ^{113}Cd NMR shifts of 1–4 in $CDCl_3$ are in the range of 440–460 ppm (Table V), consistent with the $[CdS_2N_2]$ environment around the cadmium atom.[6] The resonances for both 1 and 2 move sharply upfield upon dissolution in DMF, but no change in the chemical shift was observed in propionitrile. Attempts to recrystallize an acetonitrile adduct of either 1 or 2 were unsuccessful.

Table V. Solid-State and Solution ^{113}Cd NMR Chemical Shifts

compound	σ_{11}	σ_{22}	σ_{33}	σ_{iso}	solution δ
$Cd(S\text{-}2,4,6\text{-}i\text{-}Pr_3\text{-}C_6H_2)_2(bpy)$	814.7	629.5	31.5	491.9	448
$[Cd(S\text{-}2,4,6\text{-}i\text{-}Pr_3\text{-}C_6H_2)_2(phen)]_2$	733.7	424.1	−42.7	371.5	450
$Cd(S\text{-}2,4,6\text{-}i\text{-}Pr_3\text{-}C_6H_2)_2(1\text{-}Me\text{-}imid)_2$	787.2	528.4	135.2	483.6	457
$Cd(S\text{-}2,4,6\text{-}i\text{-}Pr_3\text{-}C_6H_2)_2(1,2\text{-}Me_2\text{-}imid)_2$	762.8	530.2	183.3	492.1	474

Table VI. Directional Cosines for $Cd(S\text{-}2,4,6\text{-}i\text{-}Pr_3\text{-}C_6H_2)_2(bpy)$

principal values	shift tensor direction cosines				reference frame direction cosines		
	a^*	b	c		a^*	b	c
σ_{11}	0.5309	0.4228	0.7344	x	0.4775	0.4190	0.7723
σ_{22}	−0.2256	−0.7648	0.6034	y	−0.3681	−0.7027	0.6088
σ_{33}	−0.8168	0.4860	0.3107	z	−0.7978	0.5750	0.1813

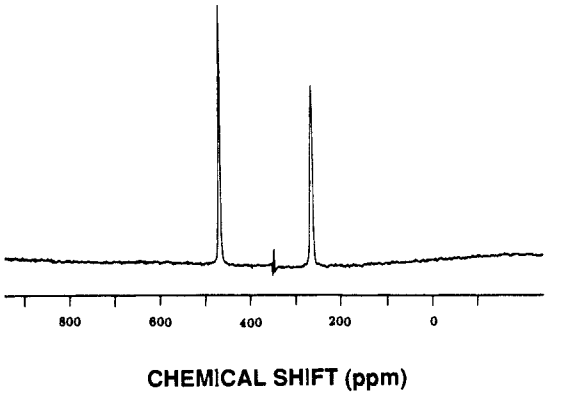

Figure 4. ^{113}Cd NMR spectrum of a single crystal of $[Cd(S\text{-}2,4,6\text{-}i\text{-}Pr_3\text{-}C_6H_2)_2(bpy)]$ (1).

Single-Crystal ^{113}Cd Nuclear Magnetic Resonance Studies. The ^{113}Cd NMR spectrum (Figure 4) of a single crystal of 1 shows two distinguishable resonances, which correspond to the two magnetically inequivalent (but chemically identical) Cd sites generated by the 2_1 symmetry operator within the unit cell.[17] The different line widths of the two resonances are presumed to be due to the anisotropy of the direct and indirect dipolar couplings to the coordinating ^{14}N atoms of the bipyridine ligands, which can cause line widths of up to 800 Hz in this compound, and occasionally resolved splittings. These splittings are, however, too small and too complex to give dipolar tensor information.

Figure 5 shows a typical rotation plot for the ^{113}Cd resonances of 1. By use of three such plots, obtained about three mutually orthogonal rotation axes, chemical shielding tensors were obtained for the two symmetry-related molecules. Although two orthogonal rotation experiments are sufficient to identify the tensor elements, the third was used as a check on the accuracy of the experimental results. From these tensor principal values and orientations, a least-squares refinement was applied to all three rotation plots for both molecules simultaneously, generating the principal values and orientations for this molecule in the goniometer reference frame. The orientation of this reference frame was established by optical goniometry. The ^{113}Cd principal values and direction cosines are given in Table VI. The directions of the principal axis systems are shown pictorially in Figure 6.

The principal axes of the ^{113}Cd NMR chemical shielding tensor and its direction cosines relative to the crystallographic axis system, a^*, b, and c, are listed in Table VI. The direction cosines of the second Cd tensor elements can be generated by a C_2 operation along b. The reference system, shown in Figure 6, is as follows: x, axis normal to the plane defined by Cd, S1, and S2; y, the imaginary bisector of the N1–Cd–N2 angle; z, the cross product of x and y, almost normal to the N1–Cd–N2 plane. The important features are as follows: (1) The least shielded element (σ_{11} = 814

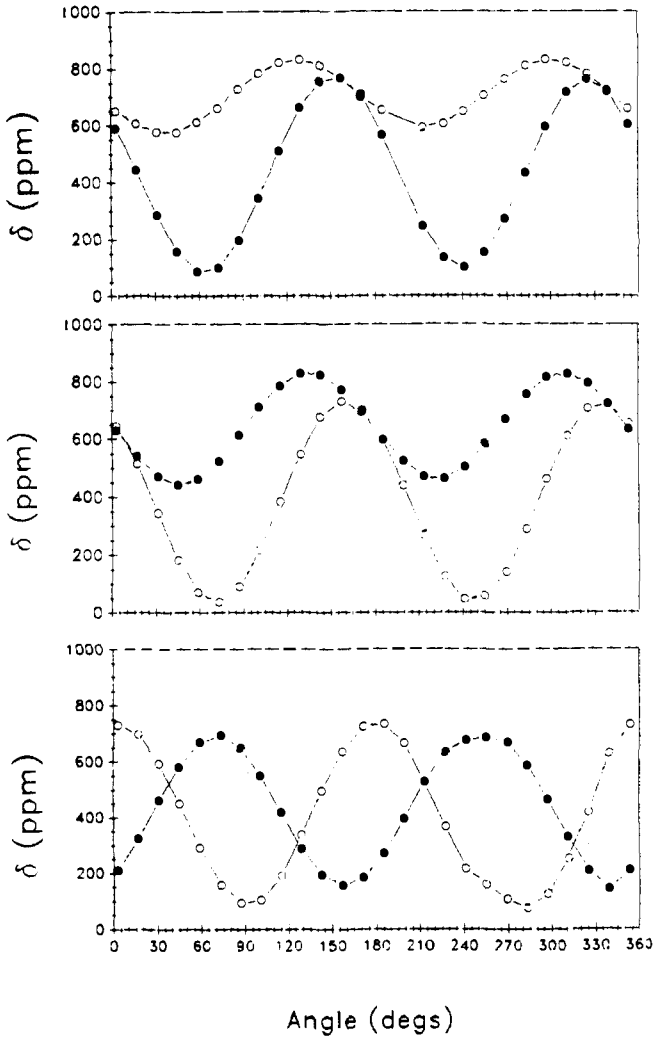

Figure 5. Orthogonal rotation plots for the ^{113}Cd NMR spectrum of a single crystal of $[Cd(S\text{-}2,4,6\text{-}i\text{-}Pr_3\text{-}C_6H_2)_2(bpy)]$ (1).

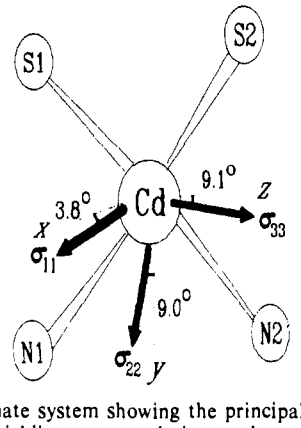

Figure 6. Coordinate system showing the principal axes of the ^{113}Cd NMR chemical shielding tensor relative to the crystallographic axis system, a^*, b, and c.

ppm) is within 9° of the x axis and makes angles of 82° and 100° with the Cd–S bonds, only slightly off from the expected 90°. (2) The σ_{22} tensor orientation is also in agreement with the expected structure–shift correlation for a CdS_2N_2 system, although the magnitude (630 ppm) is considerably larger than expected. (3) σ_{33}, the most shielded tensor element (32 ppm), lies almost along the normal to the CdN_2 bisector.

CP/MAS Spectra. Figure 7 compares the cross-polarization magic-angle spinning spectra of **1** and **2**. The large shielding anisotropies at our comparatively high field (7.1 T) cause the spectra to be broken up into centerbands and an extensive set of rotational sidebands, which are spaced by integer multiples of the

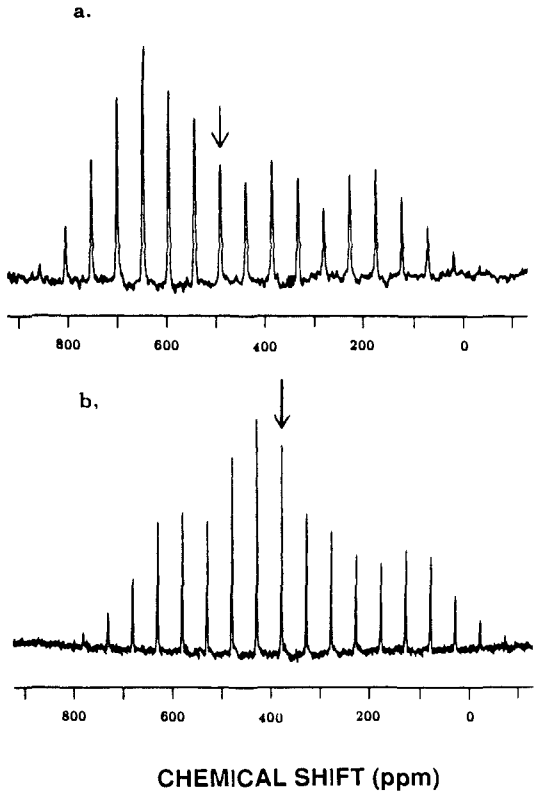

Figure 7. CP/MAS ^{113}Cd NMR Spectra of (a) $[Cd(S\text{-}2,4,6\text{-}i\text{-}Pr_3\text{-}C_6H_2)_2(bpy)]$ (1) and (b) $[Cd(S\text{-}2,4,6\text{-}i\text{-}Pr_3\text{-}C_6H_2)_2(phen)]_2$ (2) obtained at spin speeds of 3.5 and 3.4 kHz, respectively.

rotation frequency. The isotropic chemical shift frequencies are independent of the spinning speed and can easily be identified by varying the spinning rate. These resonances are marked with arrows and are separated by over 140 ppm. The differences in the shielding tensors are reflected in the quite dissimilar sideband envelopes. These dissimilarities were quantified by fitting the full sideband envelope by the method of Herzfeld and Berger.[18] The accuracy of such fits was checked by running a static spectra of **1**; the principal values obtained from the singularities in the powder pattern agreed with those from the sideband fit to within ±7 ppm. The results of these calculations are listed in Table V, where the principal values of the shielding tensors for **1**, **2**, and the two imidazole derivatives **3** and **4** are given. The isotropic chemical shift values obtained from the solid-state measurements can be compared to those in solution (Table V). It is interesting to note that no splittings due to J coupling with ^{14}N were observed for any of these compounds, despite the excellent resolution. The absence of splitting could be due to either rapid quadrupolar relaxation of the ^{14}N nucleus or a value for the J coupling of less than 150 Hz. Since apparent dipolar splittings were observed in the single-crystal experiment, the latter explanation is more likely.

The solid-state CP/MAS spectra of **1** do not add much additional information to that already obtained from single-crystal studies. Figure 7 shows the CP/MAS spectrum of **1** spinning at 3.5 kHz where the large anisotropy can clearly be seen. It is interesting to note the nearly axial symmetry of the shielding tensor, which reflects the strong deshielding environment of both nitrogen and sulfur donor ligands. There is, however, no real symmetry present in **1**.

Discussion

X-ray Crystal Structures. The solid-state structures of **1–3** present an excellent example of the effect of minor changes in ligands on metal coordination. The bipyridine and phenanthroline ligands can be considered to be almost identical in geometry and electron-donating ability; however, the solid-state structures are remarkably different. Compound **1** is monomeric and four-coordinate in the solid state, similar to but not isomorphous with $[Zn(S\text{-}2,4,6\text{-}i\text{-}Pr_3C_6H_2)_2(bpy)]$.[6d] The phenanthroline complex,

2, may be regarded as a weak dimer. The nonbridging bond distances in 2 [Cd–S_{av} 2.46 (1) Å, Cd–N_{av} 2.38 (2) Å] are not only slightly longer than those seen for 1 [2.43 (1), 2.336 (6) Å], but the geometry about the cadmium atom is distorted trigonal bipyramidal. Although the "bite angles" are almost identical for bpy and phen, the phenanthroline ligand is more rigid and therefore may impose enough of a constraint on the metal to allow the dimeric structure to form upon crystallization. The dimeric structure of 2 is similar to a previously reported cobalt complex with a less sterically hindered thiolate ligand.[6a] $[Co(S\text{-}2,3,5,6\text{-}Me_4\text{-}C_6H)_2(bpy)]_2$ exists in the solid state as a thiolate-bridged dimer with Co–S_b distances of 2.585 (2) and 2.326 (2) Å and a Co–Co distance of 3.31 Å. The cobalt complex with the S-2,4,6-*i*-$Pr_3C_6H_2$ ligand is a five-coordinate monomer with the fifth ligand coming from the solvent, $[Co(SR)_2(bpy)(CH_3CN)]$.[6a] In the cobalt series, there has been no indication of a difference between analogous bpy and phen complexes; however, the phen analogues have not been crystallographically characterized. Finally, the weak dimer seen in the solid-state structure of 2 almost certainly dissociates upon solvation, but interestingly, no evidence for coordination of nitrile solvents has been observed.

The structure of 3 is similar to the related zinc compound, $[Zn(S\text{-}2,3,5,6\text{-}Mc_4C_6H)_2(1\text{-}Me\text{-}imid)_2]$.[6d] The structure of 3 in the solid state is more closely tetrahedral than 1 and this is not surprising since it has four monodentate ligands. The Cd–S distance in 3 is 0.03 Å longer than in 1 while the Cd–N bonds in 3 are 0.07 Å shorter than the corresponding distances in 1. A similar effect has already been observed in the Zn analogues of 1 and 3.[6d] For both Zn and Cd, an increase in the M–N distance in the bpy compounds is compensated by a decrease in the M–S distance. These differences are almost certainly due to the constraint of the bpy ligand. These observations are further examples of an important structural trend in mixed-ligand complexes: individual metal ligand bond lengths are dependent on the identity of the other ligands in the coordination sphere. As expected from the increased radius of Cd^{2+}, the Cd–S and Cd–N bonds in both 1 and 3 are 0.16 and 0.22 Å longer than the related bonds in the zinc compounds. The structural similarities between analogous zinc and cadmium complexes have generally been observed in the series of tetrahedral $[M(SR)_x(N\text{-donor})_{4-x}]$ compounds.[6] These synthetic compounds provide support for the isomorphous substitution of Cd for Zn in $[Zn(S\text{-Cys})_x]$ centers in proteins.

Solution ^{113}Cd NMR Spectroscopy. The solution shifts listed in Table V for the $[Cd(SR)_2(N\text{-donor})_2]$ complexes are typical for compounds of this stoichiometry with ortho-disubstituted benzenethiolate ligands.[6b] It is interesting to note that 1 and 2 have almost identical solution chemical shifts, indicating that they both assume the same (monomeric tetrahedral) coordination geometry in solution. The difference between 3 and 4 is most likely due to the additional electron-donating ability of the 1,2-dimethylimidazole ligand, since no difference in geometry is expected.

The chemical shifts of 1 and 2 are the same in $CHCl_3$ and in propionitrile. It would thus appear that 1 and 2 do not increase their coordination number by binding nitrile solvents, as was the case for the analogous cobalt complexes. There is a considerable shift in the ^{113}Cd chemical shift in DMF compared to that in $CHCl_3$; compounds 1 and 2 shift to 382 and 323 ppm, respectively, in DMF. This result may indicate the coordination of the DMF to give five-coordinate complexes; however, the possibility of a major change in the coordination geometry in the DMF has not been ruled out.

The ^{113}Cd chemical shift of a Cd-substituted zinc finger protein with the $[M(S\text{-Cys})_2(His)_2]$ ligation has not, as yet, been measured. However ^{113}Cd NMR shift for the imidazole-inhibited catalytic site of Cd-substituted LADH with its $[Cd(S\text{-Cys})_2(His)(imid)]$ center is 518 ppm.[19] The upfield shifts of 1–4 relative to the protein can be attributed to the difference in electron-donating ability of the aliphatic (i.e., cysteine) vs aromatic thiolate ligands.

Solid-State ^{113}Cd NMR Spectroscopy. The most remarkable feature of these data is the degree to which four compounds whose solution NMR parameters are unremarkable and scarcely distinguishable from each other can differ so widely from each other in the solid state. Differences in isotropic shift of 120 ppm, arising ultimately from tensor element changes of as large as 225 ppm, are observed. These differences are apparently due to differences in the solid-state geometry, which we can analyze by referring to the crystal structures.

Single-Crystal Study. The single-crystal NMR study of the bipyridine compound, 1, reveals the orientations of the three tensor principal axes. These axes are essentially as dictated by the precepts laid down by Ellis.[20] The most deshielded axis is almost perpendicular to the bonds the cadmium atom makes with the more deshielding pair of ligands (the thiolates); the least deshielded axis makes the smallest angle with the Cd–S bonds. The principal axis directions deviate significantly from the symmetry axes of both the CdS_2 and CdN_2 planes; presumably this reflects the overall distortion of the molecule from tetrahedral symmetry.

Knowing these directions, we can begin to analyze the effect that perturbing the ligand geometry has on the Cd chemical shielding tensors. For example, since the deshielding effect of the thiolate ligands is primarily on the two downfield elements of the shielding tensor, we expect that perturbations primarily affecting these ligands (e.g., changes in the Cd–S bond length) will tend to affect these elements and, conversely, that perturbations in the CdN_2 system will primarily affect the upfield element. If we compare the shielding tensor of 1 with that of 3, these influences are obvious. The two nitrogen donor ligands in 3 are not covalently linked to each other and thus are free to adopt a much wider angle than the bipyridine ligand in 1. The less constrained coordination geometry is reflected in the shorter Cd–N bond lengths in 3 (2.26 vs 2.34 Å); the effect of these shorter bonds is reflected in a σ_{33} element that is 104 ppm further downfield in 3 compared to 1. In contrast, the average Cd–S bond length in 1 is approximately 0.03 Å *shorter*, and the σ_{11} and σ_{22} elements are correspondingly *downfield* by 25 and 100 ppm, respectively. The overall effect of the changes in the sulfur and nitrogen bond lengths almost cancel and the overall isotropic chemical shifts (the average of the three principal values) are almost identical, although it is important to note that both isotropic shifts in the solid state are significantly downfield of the solution chemical shifts.

Compound 4 appears to be isostructural with 3 and the shielding tensors are very similar. Compound 2, apparently chemically very similar to 1, has grossly different geometry and solid-state NMR properties. This compound can be regarded either as a highly distorted four-coordinate species or as a weak dimer with each cadmium atom possessing a trigonal-bipyramidal coordination geometry with one very long Cd–S bond. For the purposes of discussing the shielding tensor, it is more profitable to adopt the former viewpoint. In this compound, the Cd–N bonds are 0.04 Å longer than in 1, and as might be expected, the σ_{33} element is highly upfield shifted to over 70 ppm from what is observed in 1. Large upfield shifts are however also seen in the other two tensor elements, even with respect to 3, which has very similar Cd–S bond distances. These effects probably reflect the gross distortion of 2 away from tetrahedral symmetry; one of the nitrogen atoms is virtually coplanar with the CdS_2 plane and it is difficult even to conjecture what effect this might have on the orientations of the principal axes. Nonetheless, the overall isotropic shift is perturbed 120 ppm upfield from 1 and 90 ppm from the solution value for 2, presumably largely due to the weaker nitrogen coordination. The upfield shift also indicates that the very weakly coordinated fifth sulfur atom has a very limited effect on the solid-state chemical shift, since the influence of an additional thiolate ligand would be expected to increase the overall chemical shift. It would be useful to explore possible changes in the tensor orientation relative to 1 as a result of the structural distortions; difficulty in growing a sufficiently large single crystal has so far prevented this.

These data illustrate on one hand that a knowledge of the full chemical shielding tensor can be invaluable as a probe of the coordination geometry of tetracoordinate cadmium species, and also that simplistic interpretations based on comparing solution

chemical shifts with solid-state structures, or on speculating coordination geometries from these shifts alone, are potentially completely incorrect. Upfield shifts in one element of the shielding tensor may be canceled by opposing effects of the other elements, leading to isotropic chemical shifts whose similarity hides gross differences in stereochemistry. Given the current interest in ^{113}Cd NMR as a probe of divalent metal sites in proteins, these dangers should not be taken lightly.

The large anisotropies of the chemical shielding tensors are also of significance for the ^{113}Cd NMR of proteins and other macromolecular systems. The chemical shielding anisotropies (CSAs) reported here are among the largest yet measured for this nucleus. For cadmium with similar coordination geometry in high molecular weight systems, it is likely that CSA relaxation will have a dominant effect on line width and perhaps preclude observation of the nucleus in larger proteins and/or proteins bound to DNA. For cadmium in the solid state, high spinning speeds will be necessary to reduce the comb of sidebands exemplified by Figure 7. In both solution and solid-state NMR, the advantages of going to higher field will be minimal, since sensitivity gains will be small and resolution in solution may actually be diminished.

We are currently studying related systems to further elucidate the effects of geometry and ligand type and number on the magnitude and direction of tensor elements in the ^{113}Cd NMR spectrum. Hopefully, a meaningful set of structure–shift correlations can be established.

Conclusion

Several potential models for $[Cd(S\text{-}Cys)_2(His)_2]$ sites cadmium-substituted metalloproteins have been synthesized and characterized by X-ray crystallography and solution and solid-state ^{113}Cd NMR. A small change of nitrogen donor ligand from bipyridine to phenanthroline causes a completely different solid-state structure to be adapted, which is also reflected in the ^{113}Cd NMR chemical shift tensors. Single-crystal NMR of **1** confirms that the sulfur atoms of the thiolate ligands bound to the cadmium atom are primarily responsible for the magnitude of the least shielded tensor element (σ_{11}), but there is an unexpected and large deshielding tensor element (σ_{22}), which arises largely from the contribution of the bipyridine ligand. Preliminary studies on related compounds indicate that both σ_{22} and σ_{33} reflect the effect of the nitrogen donor ligands. The isotropic solution shifts of **1-4** are significantly different from the solid-state shifts of these compounds. This difference can be explained in the phenanthroline compound by dissolution of the dimer in solution and by a small (but significant) change in the metal–ligand bond distances for the other compounds. We are continuing the study of these $[Cd(SR)_x(N\text{-donor})_{4-x}]$ systems in order to answer these questions.

Finally, the large chemical shielding anisotropy of **1** indicates that CSA would be the likely relaxation pathway for Cd-substituted metalloproteins. This would imply a short T_2 for these systems, which would make ^{113}Cd solution NMR study more difficult. Similarly, the large CSA dictates high spinning speeds in solid-state NMR studies of such materials.

Acknowledgment. This work was supported by NIH Grants GM 31849 to S.A.K. and GM-39071 to G.S.H. and by a Presidential Young Investigator award to G.S.H. We thank Dr. George Crull for assistance with the ^{113}Cd solution NMR studies.

Supplementary Material Available: Tables of atomic coordinates, thermal parameters, bond distances, and bond angles for **1-3** (21 pages); tables of observed and calculated structure factors for **1-3** (31 pages). Ordering information is given on any current masthead page.

Highly Enantioselective Photodeconjugation of α,β-Unsaturated Esters. Origin of the Chiral Discrimination

Olivier Piva, Reza Mortezaei, Françoise Henin, Jacques Muzart, and Jean-Pierre Pete*

Contribution from the Laboratoire des Réarrangements Thermiques et Photochimiques, Unité Associée au CNRS, Université de Reims Champagne-Ardenne, U.F.R. Sciences, 51062 Reims Cédex, France. *Received March 19, 1990*

Abstract: The photodeconjugation of α-methyl conjugated esters can be highly enantioselective when carried out in CH_2Cl_2 or hexane in the presence of catalytic amounts of chiral β-amino alcohols. Enantiomeric excesses (ee %) up to 70% are described. A correspondence is established between the configuration of the new asymmetric center of the deconjugated ester and the configuration of the asymmetric carbon linked to the nitrogen of the chiral auxiliary. A model involving a nine-membered-ring transition state is proposed to rationalize the results. The effects of the reaction conditions on the level of enantioselectivity are examined. Discrimination parameters $\Delta\Delta H^{\ddagger}$ and $\Delta\Delta S^{\ddagger}$ can be determined from experiments at various temperatures. For a given ester and β-amino alcohol pair, $\Delta\Delta S^{\ddagger}$ and $\Delta\Delta H^{\ddagger}$ are shown to have the same sign which indicates that the major enantiomer corresponds to the most ordered diastereoisomeric transition state. Among the great variety of chiral β-amino alcohols used in this study, 2-(*N*-isopropylamino)-1-phenyl-1-propanol appears to be the best choice to induce high ee %. The scope and limits of the enantioselective photodeconjugation and the generality of the model are discussed.

Despite considerable efforts of organic chemists in the field of asymmetric synthesis, only a few photochemical studies have been concerned with asymmetric induction in solution, and the reported selectivities are usually quite low.[1] Among the processes available to photochemists, the photocycloaddition of chiral substrates to alkenes is very promising since diastereoselectivities higher than 80% have already been described[2] for stoichiometric amounts of the chiral inductor. A search for enantioselective photochemical reactions involving only catalytic amounts of a chiral auxiliary seems to us to be very important even if the reported selectivities

(1) (a) Rau, H. *Chem. Rev.* **1983**, *83*, 535. (b) Horner, L.; Klaus, J. *Liebigs Ann. Chem.* **1979**, 1232. (c) Kagan, H. B.; Fiaud, J. C. In *Topics in Stereochemistry*; Eliel, E. L., Allinger, N. L., Eds.; J. Wiley: New York, 1977; Vol. 10, p. 175.

(2) (a) Nehrings, A.; Scharf, H. D.; Runsink, *J. Angew. Chem., Int. Ed. Engl.* **1985**, *24*, 877. (b) Koch, H.; Scharf, H. D.; Runsink, J.; Leismann, H. *Chem. Ber.* **1985**, *118*, 1485. (c) Weuthen, M.; Scharf, H. D.; Runsink, J.; Vassen, R. *Chem. Ber.* **1988**, *121*, 971. (d) Lange, G.; Decicco, C.; Tan, S. L.; Chamberlain, G. *Tetrahedron Lett.* **1985**, *26*, 4707. (e) Lange, G.; Lee, M. *Tetrahedron Lett.* **1985**, *26*, 6163. (f) Meyers, A. I.; Fleming, S. A. *J. Am. Chem. Soc.* **1986**, *108*, 306. (g) Tolbert, L. M.; Ali, M. B. *J. Am. Chem. Soc.* **1982**, *104*, 1742. (h) Demuth, M.; Palomer, A.; Sluma, H. D.; Dey, A. K.; Krüger, C.; Tsay, Y. H. *Angew. Chem., Int. Ed. Engl.* **1986**, *25*, 1117.

0002-7863/90/1512-9263$02.50/0